

EPJ E

Soft Matter and
Biological Physics

EPJ.org
your physics journal

Eur. Phys. J. E (2013) **36**: 41

DOI 10.1140/epje/i2013-13041-0

Spin Brazil-nut effect and its reverse in a rotating double-walled drum

Decai Huang, Ming Lu, Surajit Sen, Min Sun, Yaodong Feng
and Anna Yang

edp sciences



 Springer

Spin Brazil-nut effect and its reverse in a rotating double-walled drum

Decai Huang^{1,2,a}, Ming Lu³, Surajit Sen^{2,b}, Min Sun¹, Yaodong Feng¹, and Anna Yang¹

¹ Department of Applied Physics, Nanjing University of Science and Technology, Nanjing 210094, China

² Department of Physics, University at Buffalo, State University of New York, New York 14260, USA

³ School of Chemical Engineering, Nanjing University of Science and Technology, Nanjing 210094, China

Received 11 December 2012 and Received in final form 5 March 2013

Published online: 23 April 2013 – © EDP Sciences / Società Italiana di Fisica / Springer-Verlag 2013

Abstract. The segregation of binary mixtures in a filled rotating double-walled drum is explored by simulations. Based on the characteristics of self-gravity and the centrifugal force, we argue that both percolation and buoyancy effects dominate the segregation process. The simulational results show that up to long enough times the segregation state is controlled by the rotational speed, the particle radius and density. At low rotational speeds, the smaller and heavier particles tend to accumulate towards the inner drum wall and the bigger and lighter ones towards the outer drum wall, while the segregation pattern reverses completely at higher rotational speeds. Two typical phase diagrams in the space of the density and radius ratio of bigger particles to smaller particles further confirm the predictions.

1 Introduction

A large fraction of the world's raw materials are in the form of powders and grains [1, 2]. Many of their behaviors, such as convection [3], heap formation [4], and surface wave formation [5], pose to be problems of formidable complexity. In recent literature, segregation of binary mixtures have received much attention. The segregation is usually classified by differences in particle size and particle density [6–8]. Percolation and buoyancy effects are thus proposed to explain the dynamics of systems having different sized particles (S-type systems) and particles of different densities (D-type systems). In an S-type system, the smaller particles easily sieve down through the gaps between the particles, however, in a D-type system, the heavier density particles sink earlier than the lighter ones.

In recent years, many studies have focused on rotational systems [9–11]. Different flow regimes, *e.g.*, avalanching, rolling, cascading, cataracting, and centrifuging, have been seen in these systems. The origins of these phenomena are closely related to the rotational speeds [12–14]. The Brazil-nut effect (BNE) and the Reverse Brazil-nut effect (RBNE) along the radial direction in a rotating drum are examples of complex phenomena with a strong dependence on rotational speeds [15–17]. For example, experiments show that smaller particles accumulate in a moon-like or a sun-like core of the bed and larger particles surround at the periphery at low rotational speeds.

When the rotational speed is increased to a higher value, the smaller particles tend to move towards the outer drum wall and the larger ones are driven far away from the outer drum wall. We show in a recent work that the BNE and RBNE segregation patterns can be manipulated by altering the density ratio of larger particles to smaller particles [18, 19].

In this letter, we present results on the radial segregation of binary mixtures in a rotating double-walled drum. First, we describe the simulation model and the method. The segregation degree is quantitatively defined by the segregation index to be introduced below. A theoretical argument is pursued and the effects of percolation and buoyancy on segregation are proposed. Then, a series of systems, *i.e.*, S-type system, D-type system, S+D-type system (the smaller heavy particles and the larger light particles) and S-D-type system (the smaller light particles and the larger heavy particles) are simulated to confirm the arguments. We next give a full description of the segregation states as a function of the rotational speed and plot the phase diagram in the space of density and radius ratio of bigger particles to smaller particles. The conclusion is summarized next.

2 Simulation model and method

Molecular dynamics simulations are used to explore the segregation and mixing of binary mixtures in a quasi-two-dimensional double-walled drum as shown in fig. 1. In our studies, *i.e.*, the double-walled drum has an outer wall with

^a e-mail: hdc@njust.edu.cn

^b e-mail: sen@buffalo.edu

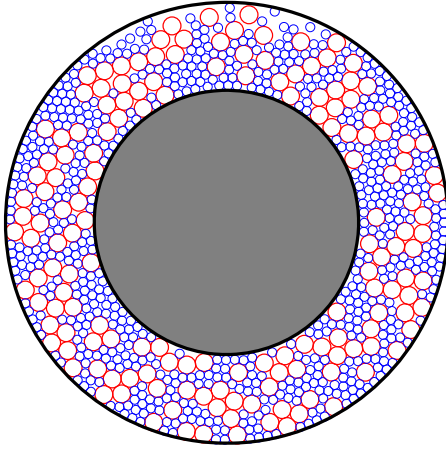


Fig. 1. (Color online). A snapshot of the system at the beginning of simulation.

diameter $D_o = 150.0$ mm and an inner wall with diameter $D_i = 90.0$ mm. The drum is $\delta_t = 1.0$ mm thick and the disks with sphere-like edges have same thickness. The inner wall is at rest at all times and the outer wall rotates clockwise. In this paper, the raining procedure is adopted to create an initial state [20]. At the beginning of the simulation, the particles are randomly placed in the upper part of the drum until no particles can get into the drum. Thus the drum is an almost fully filled condition. The particles fall under self-gravity when the rotational speed of the outer wall is set to zero. Equal volumes of the two types of particles are used. In all runs, the gravitational acceleration $g = 9.8$ m/s² and points vertically downward along the plane of the paper.

In the simulations, the dynamics of each particle is described by Newton's equations just as in our previous works [18, 19, 21, 22]. Both the translational and the rotational motions are considered. The Verlet algorithm is used to update the positions and velocities of particles. The soft sphere model is introduced to describe the interaction between the particles [23, 24]. The Kuwabara-Kono model is used for the normal interactions

$$F_{ij}^n = -k_n \xi_{ij}^{3/2} - \eta_n \xi_{ij}^{1/2} V_{ij}^n. \quad (1)$$

The tangential component is determined by the minor of the tangential force with a memory effect and the force of dynamic friction

$$F_{ij}^\tau = -\min(k_t \zeta_{ij}, \mu F_{ij}^n). \quad (2)$$

where, $\xi_{ij} = \max(0, d_{ij} - |\mathbf{x}_j - \mathbf{x}_i|)$ and $\mathbf{V}_{ij} = (\mathbf{V}_j - \mathbf{V}_i)$ denotes the particle overlap and relative velocities of two contacting particles i and j . d is the sum of radii of the contacting particles r_i and r_j and x_i and x_j are the particle positions. ζ_{ij} denotes the displacement in the tangential direction that took place since time t_0 , when the contact was first established. k_n , k_t and η_n characterize the stiffness and damping of the granular materials and are related to the collision time t_n and the masses of the grains in contact are m_i and m_j . n and τ rep-

resent the normal and tangential directions at the contact point, respectively. The detailed values are as follows: $k_n = \frac{4}{3} \frac{Y_i Y_j}{Y_i + Y_j} \sqrt{\frac{R_i R_j}{R_i + R_j}}$, $k_t = \frac{2}{7} \frac{m_i m_j}{m_i + m_j} \left(\frac{\pi}{t_n}\right)^2$, $Y = \frac{E}{1-\nu^2}$, $t_n = 3.21 \left(\frac{m_i m_j}{m_i + m_j}\right)^{\frac{2}{5}} (V_{ij}^n)^{-\frac{1}{5}}$. E is the Young modulus, ν the Poisson ratio. The coefficient of sliding friction between particles is set to $\mu = 0.5$ [9]. The collisions between the particles and the inner (outer) drum wall in the radial direction are treated as particle-particle collisions, except that the drum has an infinite mass and the diameter of outer and inner drum walls are D_o and D_i , respectively.

Taking advantage of the numerical simulation, the center position of the masses is directly calculated, $h_p = \frac{1}{N_p} \sum_{i=1}^{N_p} z_i$. The angular speed of the masses is $\omega_p = \frac{1}{N_p} \sum_{i=1}^{N_p} \omega_i$. Here, p is the species of particles and N_p is the total number of p species of particles. z_i is the radial distance of particle i with respect to the inner wall edge of the drum. ω_i is the angular velocity of particle i . In order to have a quantified description of the degree of segregation, the segregation index χ is introduced [25]

$$\chi = 2.0 \frac{h_b - h_s}{h_b + h_s}. \quad (3)$$

In eq. (3), h_b and h_s are the center positions of the bigger particles and the smaller particles, respectively. As a comparison with the segregation in a vertically vibrated container [6, 26], we call the segregated state as the Brazil-nut effect (BNE), in which the smaller particles migrate towards the inner wall of the drum and the bigger ones towards the outer wall of the drum. If the segregated state is reversed, *i.e.*, the bigger particles accumulate towards the inner wall of the drum and the smaller ones towards the outer wall of the drum, the corresponding segregated state is named the Reverse Brazil-nut effect (RBNE). The BNE happens for a positive χ and the RBNE for a negative χ according to eq. (3).

3 Theoretical arguments

In the rotating-drum system, both self-gravity and centrifugal force have been found to play critical roles on particle dynamics [12, 13, 15–19]. The central purpose of this paper is to consider the segregation of binary mixtures for a broader range of rotational speeds. At low rotational speeds, the centrifugal force is so small that self-gravity dominates the dynamics. The system is in the avalanching or rolling regime. In this condition, the inner wall serves as a bottom and the particles in the surface form a flowing layer. At high rotational speeds, the centrifugal force has a larger effect than self-gravity on the dynamics of particles. The system goes in the centrifugal regime and so spin segregation happens in the radial direction. This case leads to the particles adjacent to the inner drum wall becoming the flowing layer and the outer wall working like a bottom region.

Based on the features of self-gravity and the centrifugal force, two kinds of mechanisms *i.e.*, the percolation effect and the buoyancy effect, can be used to predict what segregation patterns of binary mixtures will transpire. For an S-type system, due to the effect of percolation, the smaller particles easily sieve down through the interstices and migrate to the bottom region, *i.e.*, to the inner wall of the drum at low rotational speed and to the outer wall of the drum at high rotational speed. The larger particles are then pushed to the opposite direction leading to segregation. On the other hand, for a D-type system, the buoyancy effect drives the heavier density particles to the bottom region in sharp contrast to those with lighter density. So the layers around the inner wall and the outer drum wall are normally occupied by the heavier and lighter particles, respectively, at low rotational speeds. The reverse segregation pattern happens, *i.e.*, the regions of the outer wall and the inner wall are destinations of the heavier and lighter particles, respectively, at high rotational speeds. Therefore, the segregation states in the S+D-type system and the S-D-type system can be interpreted by using the combined effects of percolation and buoyancy. Both effects help improve the segregation of binary mixtures and a more segregated state can appear for an S+D-type system whenever the rotational speed is low or high. The only difference is that the segregation pattern is completely opposite. The smaller and heavier particles migrate to the inner drum wall at low rotational speeds and to the outer drum wall at high rotational speeds. In the S-D-type system the two effects compete with each other and the final segregation state is decided by the dominant effect. For example, at low rotational speeds, if the percolation effect overcomes the buoyancy effect, the BNE happens, and if the latter dominates, the RBNE occurs. When the two effects are equally dominant, a mixed state emerges.

In addition, there is a special case for higher rotational speeds. Due to the large centrifugal forces, the particles obtain high velocities within the first few rotations and they get firmly compacted together and rotate with the outer wall. This results in no relative motion between the particles. Thus no further segregation happens.

4 Simulational results

To confirm the above arguments, the simulations are first performed for an S-type system where the particles are of the same density but differ in size. Figure 2 shows the temporal evolution of the center position of particles with respect to the inner wall of drum at two different rotational speeds, $\omega = 30.0$ and 150.0 s^{-1} . At low rotational speeds, the smaller particles migrate towards the inner wall ($h_s = 9.86 \text{ mm}$) and the bigger particles move towards the outer wall ($h_b = 21.92 \text{ mm}$). At larger rotational speeds, the segregation condition turns over completely due to the buoyancy effect. The smaller particles are pushed towards the outer wall ($h_s = 21.28 \text{ mm}$) and the bigger particles accumulate towards the inner wall ($h_b = 12.01 \text{ mm}$). The two panels show snapshots of the

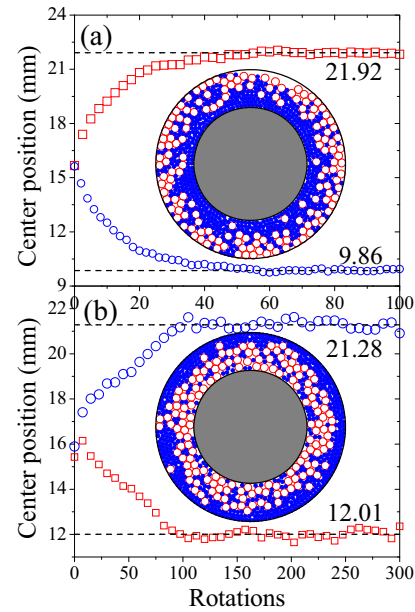


Fig. 2. (Color online). Temporal evolution of the center position of particles with respect to the inner wall of drum in the S-type system is shown. The rotational speeds are for (a) $\omega = 30.0 \text{ s}^{-1}$ and (b) $\omega = 150.0 \text{ s}^{-1}$, respectively. The red square and blue circle symbols are results for bigger particles $r_b = 3.0 \text{ mm}$ and smaller particles $r_s = 1.5 \text{ mm}$, respectively. The densities of both bigger particles and smaller particles are of the same value, $\rho_b = \rho_s = 1.0 \times 10^3 \text{ kg/m}^3$. The two insets show the snapshots of the system. The red open symbols and the blue solid symbols denote the bigger particles and smaller particles, respectively.

segregation of particles with different sizes. The two ring-like spin segregation patterns are just opposite in the radial direction. At smaller rotational speeds, the Brazil-nut effect is seen, in which the smaller particles accumulate near the inner ring and the larger particles near the outer ring. At higher rotational speeds, the Reverse Brazil-nut effect occurs, in which the inner ring has larger particles and the outer ring has smaller particles. These observations are in keeping with our arguments. We find that the percolation effect dominates the segregation process. The inner and outer walls act as the bottom regions respectively at the low and high rotational speeds.

A D-type system is then simulated, in which the particles are of the same size ($r_h = r_l = 1.5 \text{ mm}$), but the densities of heavy particles and light particles are set to $\rho_h = 5.0 \times 10^3 \text{ kg/m}^3$ and $\rho_l = 1.0 \times 10^3 \text{ kg/m}^3$, respectively. In this case, the buoyancy effect dominates the segregation process. The temporal evolution of the center position of particles with respect to the inner wall of the drum are shown in fig. 3 at two different rotational speeds, $\omega = 30.0$ and 150.0 s^{-1} . The results show that the heavy particles accumulate around the inner drum wall ($h_h = 9.87 \text{ mm}$) and the light particles are near the outer wall ($h_l = 21.88 \text{ mm}$) at the low rotational speed. When the rotational speed is increased to the high value, the heavy particles move towards the outer wall

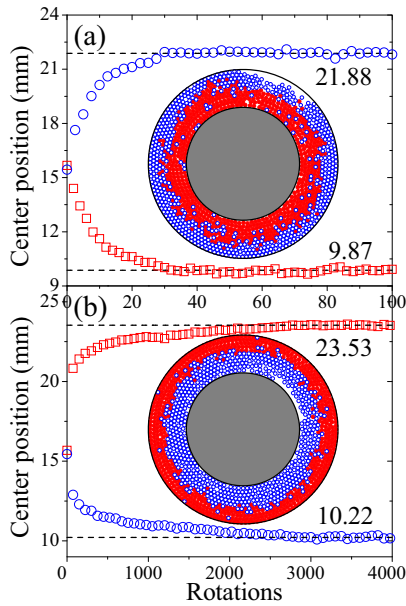


Fig. 3. (Color online). Temporal evolution of the center position of particles from the inner wall of drum in the D-type system is shown. The rotational speeds are for (a) $\omega = 30.0 \text{ s}^{-1}$ and (b) $\omega = 150.0 \text{ s}^{-1}$, respectively. The red square and blue circle symbols are results for heavier particles $\rho_h = 5.0 \times 10^3 \text{ kg/m}^3$ and lighter particles $\rho_l = 1.0 \times 10^3 \text{ kg/m}^3$, respectively. The radii of both bigger particles and smaller particles are of the same value, $r_h = r_l = 1.5 \text{ mm}$. The two insets show the snapshots of the system. The red solid symbols and the blue open symbols denote the heavier particles and lighter particles.

($h_h = 23.53 \text{ mm}$) and the light particles move towards the inner wall ($h_l = 10.22 \text{ mm}$). The corresponding two inverse ring-like spin segregation patterns are displayed directly in the two insets. For the low rotational speed, the inner ring is occupied by heavy particles and the outer ring by light particles. For the high rotational speed, the heavy particles and the light particles exchange their positions. The heavy particles move towards the outer ring and the light particles towards the inner ring.

To probe the whole segregation pattern, more complicated systems, *i.e.*, the S+D-type system and the S-D-type system, are investigated. The radii of bigger particles and smaller particles are fixed to $r_b = 3.0 \text{ mm}$ and $r_s = 1.5 \text{ mm}$, respectively, and then the density ratio of bigger particles to smaller ones is altered. Figure 4(a) and (b) show the segregation patterns of an S+D-type system at rotational speeds, $\omega = 30.0$ and 150.0 s^{-1} . For this S+D type system the densities of the bigger particles and the smaller ones are set to $\rho_b = 1.0 \times 10^3 \text{ kg/m}^3$ and $\rho_s = 5.0 \times 10^3 \text{ kg/m}^3$, respectively. We can see that the Brazil-nut effect happens at low rotational speeds, and the Reverse Brazil-nut effect occurs at high rotational speeds. The segregation patterns of an S-D-type system are shown in fig. 4(c) and (d) for rotational speeds, $\omega = 30.0$ and 150.0 s^{-1} , respectively. The densities of bigger particles and smaller ones are set to $\rho_b = 5.0 \times 10^3 \text{ kg/m}^3$ and $\rho_s = 1.0 \times 10^3 \text{ kg/m}^3$. It is notable that the Reverse Brazil-

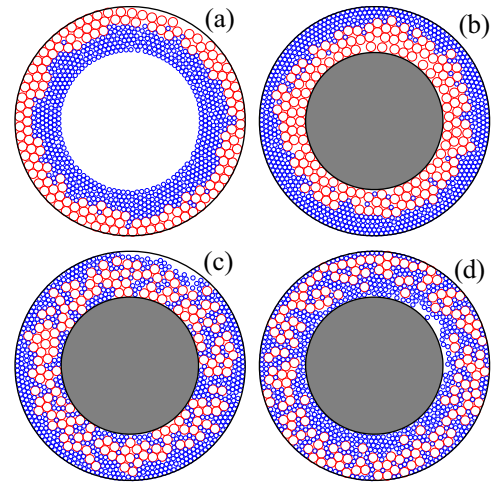


Fig. 4. (Color online). Segregation patterns for (a), (b) the S+D-type system and (c), (d) the S-D-type system are shown. The rotational speeds are set to (a), (c) $\omega = 30.0 \text{ s}^{-1}$ and (b), (d) $\omega = 150.0 \text{ s}^{-1}$. The radii of bigger particles and smaller particles are set to $r_b = 3.0 \text{ mm}$ and $r_s = 1.5 \text{ mm}$. In the S+D-type system, the densities of bigger particles and smaller ones are set to $\rho_b = 1.0 \times 10^3 \text{ kg/m}^3$ and $\rho_s = 5.0 \times 10^3 \text{ kg/m}^3$. In the S-D-type system, the densities of bigger particles and smaller ones are set to $\rho_b = 5.0 \times 10^3 \text{ kg/m}^3$ and $\rho_s = 1.0 \times 10^3 \text{ kg/m}^3$.

nut effect appears at the low rotational speed, and the Brazil-nut effect arises at the high rotational speed.

So far, we have got agreement between the arguments presented and the simulated results for the segregation of a binary mixture in the double-walled rotational system. To give a quantitative description of spin BNE and RBNE segregation, fig. 5 presents results of the segregation index as a function of the rotational speed for three systems, *i.e.*, an S-type system (\square), an S+D-type system (\triangle) and an S-D-type system (∇). For the S-type system, χ is larger than zero and the segregation pattern yields the BNE at the low rotational speed. When χ is less than zero, the segregation pattern yields the RBNE at the high rotational speed. When the rotational speed is increased to a very large value, χ is around zero, which means that the system is at an almost mixed state. For the S+D-type system, a trend similar to that in the S-type system is obtained at the low rotational speeds except that the segregation is more pronounced.

We can see that the corresponding absolute values of χ in the S+D-type system are comparatively larger than that of the S-type system at low and high rotational speeds. The S+D-type system still stays at the RBNE state when the rotational speed is increased to larger values. For the S-D-type system, the reverse segregation patterns happen. The RBNE appears at low rotational speeds and the BNE occurs at high rotational speeds. The system goes in the mixed state for high rotational speeds.

Figure 6 plots the segregation phase diagram in ρ_b/ρ_s - r_b/r_s space at the low and high rotational speeds, $\omega = 30.0$ and 150.0 s^{-1} . The BNE and the RBNE are indicated by the symbols shown in fig. 6. The solid lines give the boundaries of the BNE and the RBNE, where the absolute values

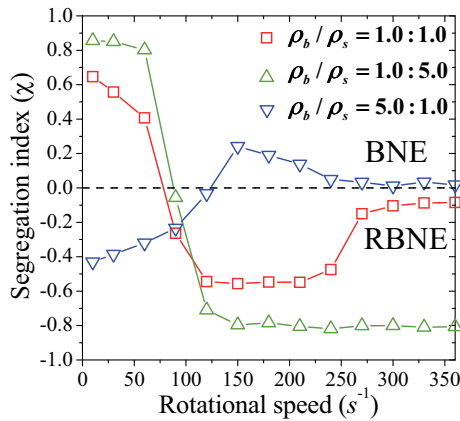


Fig. 5. (Color online). The segregation index as a function of the rotational speed is shown. The radii of bigger particles and smaller particles are set to $r_b = 3.0$ mm and $r_s = 1.5$ mm. The density ratios of bigger particles to smaller particles are set to $\rho_b/\rho_s = 1.0:1.0$ (the S-type system, \square), $1.0:5.0$ (the S+D-type system, \triangle) and $5.0:1.0$ (the S-D-type system ∇). The dashed line corresponds to the boundary of BNE and RBNE. The solid lines are guides to the eye.

of χ are actually very small and the corresponding states are almost mixed. For the low rotational speed, we can see that the BNE appears at the upper left region and the RBNE occurs at the low right region as shown in fig. 6(a). Furthermore, the boundary of the BNE and the RBNE shifts to the right when the density ratio of bigger particles to smaller ones is increased. This result implies that both the lower ρ_b/ρ_s and the larger r_b/r_s are helpful to form the RBNE, and the higher ρ_b/ρ_s and the smaller r_b/r_s to the BNE. Figure 6(b) shows that the segregation conditions turn over completely when the rotational speed is increased to the higher value. The upper left region is occupied by the BNE and the lower right one by the RBNE. Similarly, the boundary moves right when the density ratio of bigger particles to smaller ones increases. It means that the RBNE will be reinforced for lower ρ_b/ρ_s and larger r_b/r_s , and the BNE for higher ρ_b/ρ_s and smaller r_b/r_s .

5 Conclusions

The segregation of binary mixtures in a rotating double-walled drum is studied by numerical simulations. A ring-like spin segregation pattern in the radial direction can be controlled by the rotational speed and particle's radius and density. We first make the following argument. Both the percolation effect and the buoyancy effect are used to explain the segregation process of binary mixtures in the rotating drum. The percolation effect means that the smaller sized particles find it easier to go down through the interstices between the particles. The buoyancy effect facilitates the higher density particles to sink down faster compared to the lighter ones. At low rotational speeds, self-gravity dominates the particle's motion and the inner wall serves as the bottom layer. At high rotational

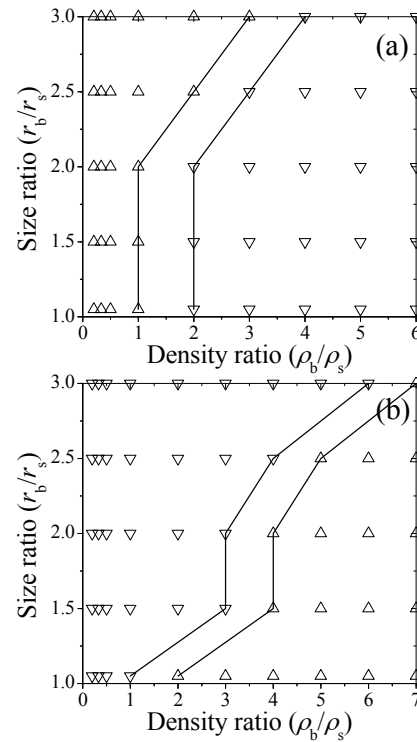


Fig. 6. Phase diagrams of the binary mixtures in the ρ_b/ρ_s - r_b/r_s space are shown for different rotational speeds. The rotational speeds are set to (a) $\omega = 30.0$ and (b) 150.0 s $^{-1}$, respectively. The upward-pointing triangles and downward-pointing triangles represent the segregation patterns of the Brazil-nut effect and the Reverse Brazil-nut effect. The solid lines show the boundaries of two segregation patterns.

speeds, the centrifugal force dominates the dynamics of the particles and the outer wall works as the bottom layer. Therefore, for the S-type, the D-type and the S+D-type systems, the Brazil-nut effect happens at low rotational speeds and the Reverse Brazil-nut effect occurs at high rotational speeds because both the percolation effect and the buoyancy effect have a positive effect on the segregation. For the S-D-type system, the two effects act in opposite directions and hence the segregation condition depends on the dominant one.

The simulations show that at low rotational speeds, the smaller and heavier particles tend to accumulate around the inner drum wall and the bigger and lighter ones accumulate adjacent to the outer drum wall. While, at high rotational speeds, the segregation pattern reverses completely and the two types of particles exchange their positions, *i.e.*, the smaller sized and higher density particles migrate towards the outer drum wall and the larger and lighter ones towards the inner drum wall. By introducing the segregation index, we quantify the dependence of the segregation state on the rotational speed and plot the phase diagram of segregation in the ρ_b/ρ_s - r_b/r_s space. All our simulation results are in good agreement with the theoretical-argument-based expectations. The results reveal new insights into the mixing processes of two-species granular systems in rotating drums.

This work was financially supported by the Young Scientists Fund of the National Natural Science Foundation of China (Grant No. 10904070), the National Natural Science Foundation of China (Grant No. 10847146), and the China Scholarship Council (Grant No. 2009307172). SS was supported by the US Army Research Office.

References

1. H.M. Jaeger, S.R. Nagel, R.P. Behringer, *Rev. Mod. Phys.* **68**, 1259 (1996).
2. I.S. Aranson, L.S. Tsimring, *Rev. Mod. Phys.* **78**, 641 (2006).
3. T. Pöschel, H.J. Herrmann, *Europhys. Lett.* **29**, 123 (1995).
4. Y. Grasselli, H.J. Herrmann, *Granular Matter* **3**, 201 (2001).
5. H.K. Pak, R.P. Behringer, *Phys. Rev. Lett.* **71**, 1832 (1993).
6. D.C. Hong, P.V. Quinn, S. Luding, *Phys. Rev. Lett.* **86**, 3423 (2001).
7. A.P.J. Breu, C.A. Ensner, I. Rehberg, *Phys. Rev. Lett.* **90**, 014302 (2003).
8. A. Kudrolli, *Rep. Prog. Phys.* **64**, 209 (2004).
9. G. Juárez, P.F. Chen, R.M. Lueptow, *New J. Phys.* **13**, 053055 (2011).
10. P.F. Chen, B.J. Lochman, J.M. Ottino, R.M. Lueptow, *Phys. Rev. Lett.* **102**, 148001 (2009).
11. S.W. Meier, D.A. Barreiro, J.M. Ottino, R.M. Lueptow, *Nat. Phys.* **4**, 244 (2008).
12. R.Y. Yang, A.B. Yu, L. McElroy, J. Bao, *Powder Technol.* **188**, 170 (2008).
13. P.F. Chen, J.M. Ottino, R.M. Lueptow, *New J. Phys.* **13**, 055021 (2011).
14. K. Yamane, M. Nakagawa, S. Altobelli, T. Tanaka, Y. Tsuji, *Phys. Fluids* **10**, 1419 (1998).
15. N. Nityanand, B. Manley, H. Henein, *Metal. Trans. B* **17**, 247 (1986).
16. K.M. Hill, G. Gioia, D. Amaravadi, *Phys. Rev. Lett.* **93**, 224301 (2004).
17. N. Jain, J.M. Ottino, R.M. Lueptow, *Granular Matter* **7**, 69 (2005).
18. D.C. Huang, M. Lu, G. Sun, Y.D. Feng, M. Sun, H.P. Wu, K.M. Deng, *Phys. Rev. E* **96**, 031305 (2012).
19. D.C. Huang, Y.D. Feng, W.M. Xie, M. Lu, M. Sun, H.P. Wu, *Acta Phys. Sin.* **61**, 124501 (2012).
20. L. Vanel, D. Howell, D. Clark, R.P. Behringer, *Phys. Rev. E* **60**, R5040 (1999).
21. D.C. Huang, G. Sun, K.Q. Lu, *Phys. Rev. E* **74**, 061306 (2006).
22. D.C. Huang, G. Sun, K.Q. Lu, *Phys. Lett. A* **375**, 3375 (2011).
23. G. Kuwabara, K. Kono, *Jpn. J. Appl. Phys.* **26**, 1230 (1987).
24. J. Schäfer, S. Dippel, D. E Wolf, *J. Phys. I* **6**, 5 (1996).
25. M.P. Ciamarra, M.D. De Vizia, A. Fierro, M. Tarzia, A. Coniglio, M. Nicodemi, *Phys. Rev. Lett.* **96**, 058001 (2006).
26. T. Schnautz, R. Brito, C.A. Kruelle, I. Rehberg, *Phys. Rev. Lett.* **95**, 028001 (2005).